Eur. Phys. J. C (2025) 85:1329
https://doi.org/10.1140/epjc/s10052-025-14776-9

THE EUROPEAN PHYSICAL JOURNAL C

Regular Article - Experimental Physics

Deuteron identification via time of flight with LHCb

LHCb Collaboration[⋆]

CERN, 1211 Geneva 23, Switzerland

Received: 8 August 2025 / Accepted: 10 September 2025

Abstract It is shown that the timing capabilities of the LHCb detector operated during the LHC Run 2 can be used to identify light ion particles with momenta of a few GeV/c. This is achieved by estimating the particle time of flight through a newly developed technique. A dedicated reconstruction procedure and a neural-network-based estimator of the particle speed have been developed to enable deuteron identification by suppressing the abundant background from lighter particles. The performance of the identification procedure is demonstrated in a sample of proton-helium collisions at $\sqrt{s_{\rm NN}}$ = 110 GeV, where the production of deuteron and triton particles is observed. This novel approach opens the way to study deuteron and antideuteron production for different collision systems at different energy scales, exploiting the rich dataset collected by the LHCb experiment.

1 Introduction

The measurement of antimatter in cosmic rays is a sensitive probe of physics beyond the Standard Model, as dark matter annihilation or decay could contribute to the flux of cosmic antiparticles [1]. The AMS-02 experiment [2] has reported several antideuteron and antihelium candidates whose origin is still unclear [3]. These particles could be produced in collisions between cosmic rays and the interstellar medium via coalescence of secondary antibaryons. While measurements of the related production cross sections have been performed at RHIC and LHC hadron colliders for a nucleon-nucleon centre-of-mass energy $\sqrt{s_{\rm NN}}$ well above 100 GeV, very limited data exist for the energy scale relevant to the AMS-02 observations, namely $\sqrt{s_{\rm NN}}$ between 10 and 100 GeV.

The LHCb detector [4,5] is a single-arm forward spectrometer covering the pseudorapidity range $2 < \eta < 5$, designed for the study of heavy-flavour particles in proton-proton (pp) collisions. During the LHC Run 2, it was also operated with pPb and PbPb collisions. Production studies in beam-beam collisions at the LHCb experiment can complement those from the other LHC detectors, which mostly cover central rapidity. Moreover, thanks to the SMOG gas target [6], the LHCb experiment also collected a rich dataset of fixed-target collisions of proton and lead beams on He, Ne and Ar targets, at $\sqrt{s_{\rm NN}}$ between 68 and 110 GeV [7].

The detector includes two ring-imaging Cherenkov (RICH) detectors that are able to discriminate between different species of charged hadrons, while leptons, photons and neutral hadrons are identified by a calorimeter system and a muon system consisting of five stations. Though light ion identification was not among the requirements of the detector design, the AMS-02 observation motivated an effort to identify light nuclei from the available detector information. In particular, a recent study has demonstrated that helium nuclei can be identified via their characteristic energy loss in the tracking detectors [8]. This recent development opens a promising avenue for light ion identification at LHCb, despite not being part of the initial design goals.

Active deuteron[1] identification in the RICH detectors is possible only for momenta above 35 GeV/c and is limited by the abundant pion background [9]. In this paper, the identification of low-momentum deuteron particles through a time-of-flight measurement is studied.

The LHCb Outer Tracker (OT) [10] consists of 12 double layers of straw tubes, arranged in three stations placed downstream of the spectrometer's magnet, at a distance between 7.9 m and 9.4 m from the nominal beam-beam collision point. Its large area covers the outer region of the spectrometer's acceptance, corresponding to particles of lower rapidity and momentum. For the LHC Run 2, the detector was precisely recalibrated, reaching an average resolution on the drift time of 2.4 ns per hit [11]. For an average number of 18 OT hits per track, the resolution for the time-of-flight measurement is therefore 0.57 ns, allowing, in principle, to distinguish

[1] The inclusion of charge-conjugated particles is implied in the following, unless otherwise stated.

⋆ e-mail: chiara.lucarelli@cern.ch

Published online: 19 November 2025

the proton and deuteron hypotheses by more than 3 standard deviations for momenta below 4.6 GeV/c. The first muon station (M1), located between the OT and the calorimeters, detects charged particles with an efficiency above 98.5% and provides an additional independent measurement of the particle time of flight with a resolution below 4 ns [12]. The timing capabilities of the OT and of M1 detectors form the basis of the technique presented in this paper.

The paper is organised as follows: a dedicated track reconstruction procedure in the OT, needed to efficiently reconstruct the deuteron candidates, is presented in Sect. 2. The strategy used to determine the particle velocity and suppress the background to deuteron identification is discussed in Sect. 3. In Sect. 4, the achieved performance of the identification procedure is presented on a sample of pHe collisions collected at $\sqrt{s_{\rm NN}}$ =110 GeV. Finally, in Sect. 5 the conclusions summarizing the performance and general applicability of the proposed method are presented.

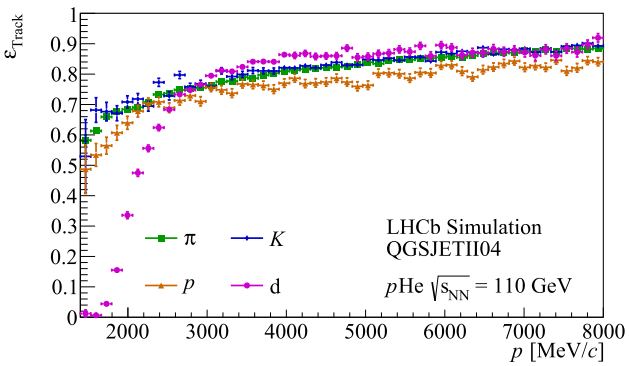

Fig. 1 Track reconstruction efficiency $\varepsilon_{\rm Track}$ of the standard pattern recognition algorithm as a function of the momentum p for different hadron species in the QGSJET-based simulation sample

2 Deuteron reconstruction

In the standard track reconstruction procedure used in the LHCb experiment (see Ref. [13] for a detailed description), candidates for particles produced at the primary collision and crossing the LHCb spectrometer are obtained through a pattern recognition algorithm known as Forward Tracking [14]. The algorithm extrapolates track segments reconstructed in the vertex detector and searches for detector hits in the other tracking stations. Hits in the OT are obtained by combining the known wire position of each OT straw tube with the measured drift time of the signals. The drift times are determined after taking into account the particle time of flight according to its trajectory from the nominal beam–beam collision point to the hit position, assuming that the particle travels at the speed of light c. For particles travelling at lower speed ($\beta = v/c < 1$), the delay of the particle arrival at the OT with respect to the ultrarelavistic hypothesis biases the reconstructed drift times. It has been shown in Ref. [11] that the average time residual of OT hits with respect to the fitted track provides some discrimination power between protons and pions. The overestimation of the drift time for particles with $\beta \ll 1$ produces a bias to their reconstructed positions in the OT. Moreover, in the standard reconstruction, late OT hits are discarded if they are compatible with being produced by a collision following the acquired one by 25 ns, given the nominal 40 MHz collision rate. The quality of the reconstructed tracks for such "slow" particles is therefore degraded, possibly causing the track candidates to be rejected.

To evaluate this effect and benchmark an improved deuteron reconstruction, three simulation samples are produced. In the first sample, single deuteron particles with momentum between 1 and 15 GeV/c are simulated in the detector. In the other samples, a more realistic simulation of pHe collisions at $\sqrt{s_{\rm NN}}$ =110 GeV is performed, requiring the presence of a deuteron in the final state. Collisions are generated using two different models, QGSJETII04 [15] or PYTHIA 6.4 [16], providing different predictions for the baryon production. Only the former includes baryon production through fragmentation of the target He nucleus. Deuteron production via coalescence of produced baryons is not included in either model and is simulated through an additional custom algorithm, similar to that described in Ref. [17]. The interaction of the generated particles with the detector, and its response, are implemented using the GEANT4 toolkit [18,19] as described in Ref. [20].

The efficiency of the standard LHCb pattern recognition algorithm for different hadron species in simulated events is shown in Fig. 1. It is computed for particles in the detector acceptance that produce enough detector hits to be possibly reconstructed. The efficiency for deuterons is strongly degraded for momenta below 3 GeV/c, namely in the most promising kinematic region for deuteron identification via time of flight.

A modified version of the pattern recognition algorithm, named TofForward hereafter, is developed to recover the slow deuteron candidates. All recorded OT hits are considered, including late signals that could be produced by low-momentum deuterons. In an initial step, the Forward Tracking algorithm is performed without using the drift-time information, reconstructing the hit positions from the centre of the straw tubes with an uncertainty equal to their radius. This selects candidates that can be reconstructed independently of the assumed particle speed and provides a first estimation of the particle momentum. The drift-time information is then added and the Forward Tracking is repeated for different hypotheses on the particle velocity. Explored values of β range from 1 to the value corresponding to a

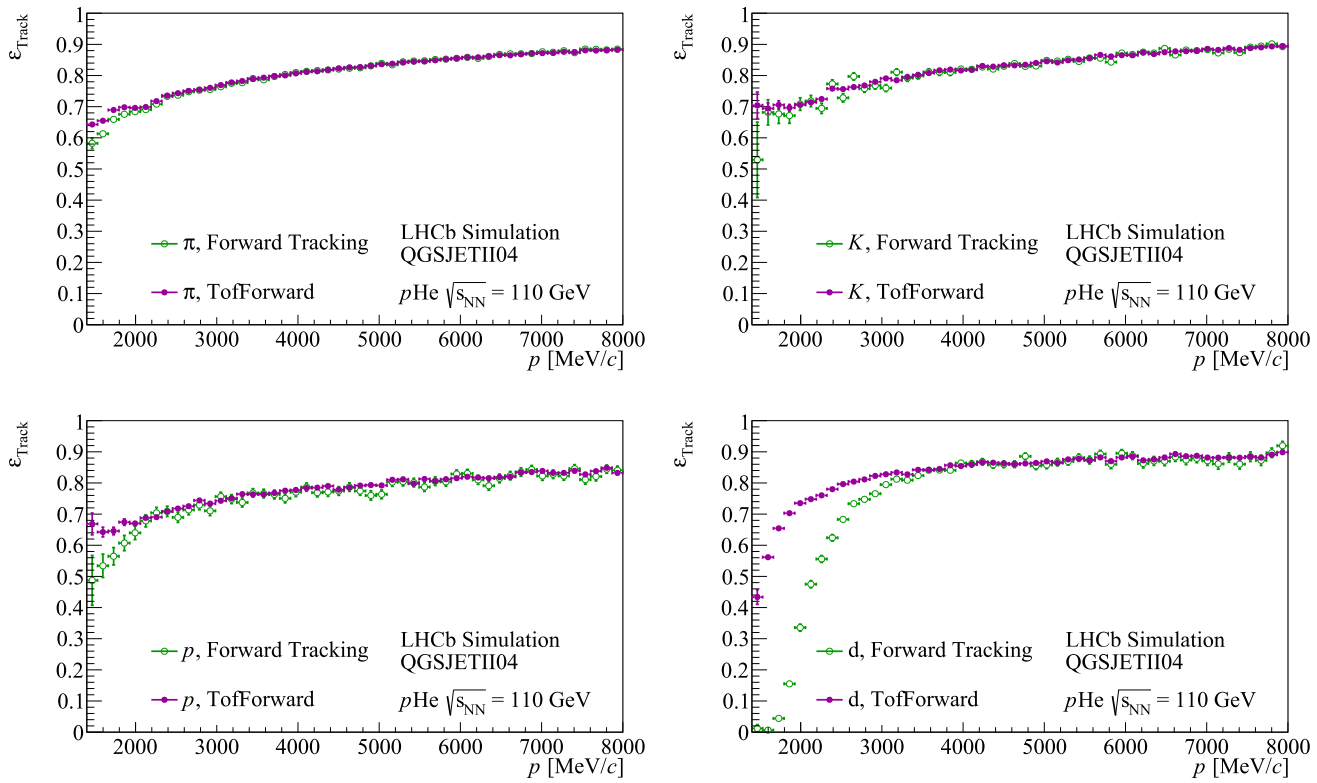

Fig. 2 Track reconstruction efficiency as a function of the momentum for (top left) pions, (top right) kaons, (bottom left) protons and (bottom right) deuterons; the performance of (empty markers) the standard Forward Tracking algorithm and of (full markers) the TofForward algorithm is compared

^{4}He nucleus with momentum equal to the initial estimate, in steps of 0.05. The latter value is chosen as a compromise between the highest tracking efficiency and the minimum computing time. The track candidate is obtained from a fit minimising the χ^2 of the spatial residuals of the hits associated with the track and the β value corresponding to the minimum fit χ^2 is assigned to the candidate. The quality requirements on the candidates are simplified by omitting the neural-network-based selection [21], which is used in the standard procedure and optimised for high-momentum particles.

The tracking efficiency obtained with the TofForward algorithm is compared to the standard reconstruction in Fig. 2. A significant improvement is achieved for deuterons (protons) with momenta below 4 GeV/c (2 GeV/c). The momentum resolution, being dominated at low momentum by multiple scattering, is found to be comparable between the two algorithms, see Fig. 3. To verify that the looser selection is not affecting the quality of the reconstructed track sample, the rate of so-called ghost tracks, namely candidates built combining hits from different particles, as a function of the event multiplicity, measured as the number of reconstructed tracks (nTracks) in the event, is also compared in Fig. 3. No significant difference is observed between the two algorithms.

3 Measurement of the particle speed

In the LHCb track reconstruction procedure, the track candidates obtained from the pattern recognition algorithm are refitted using an algorithm based on a Kalman filter [22] to achieve a refined determination of the particle kinematics by taking into account multiple scattering and energy loss effects.

This algorithm is extended to be able to estimate β, using the simulated sample of standalone deuterons as a test-bench. A given β value is tested by running the Kalman filter after correcting the OT reconstructed drift times for the expected particle time of flight along its reconstructed trajectory, assuming that the particle is produced at the position of closest approach to the nominal beam line. The β estimation is obtained by minimising the track χ^2 of the Kalman filter plus the normalised residual of the time measurement in the first muon station M1,

$$\chi^2_\beta(\beta) = \chi^2_{\text{Kalman}}(\beta) + \left[\frac{t_{\text{M1}} - t_{\text{M1,exp}}(\beta)}{\sigma_{\text{M1}}}\right]^2, \quad (1)$$

where t_{M1} is the observed time in M1 and $t_{\text{M1,exp}}$ its expected value for a given β hypothesis; $\sigma_{\text{M1}} = 4$ ns is the M1 time resolution.

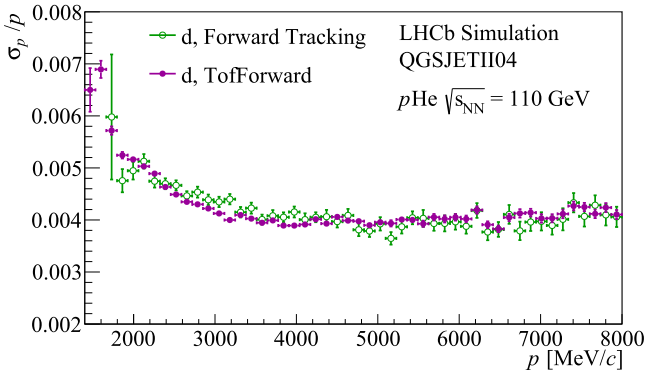

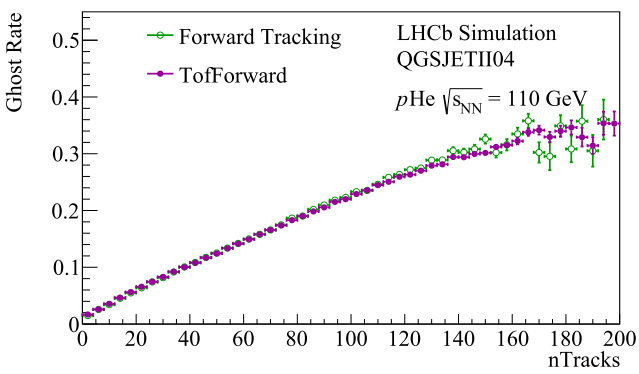

Fig. 3 (Left) Momentum resolution as a function of the momentum for deuterons in the QGSJET-based simulation sample for (empty markers) the standard Forward Tracking algorithm and (full markers) the TofForward algorithm. (Right) Average number of ghost tracks as a function of the reconstructed track multiplicity is also compared

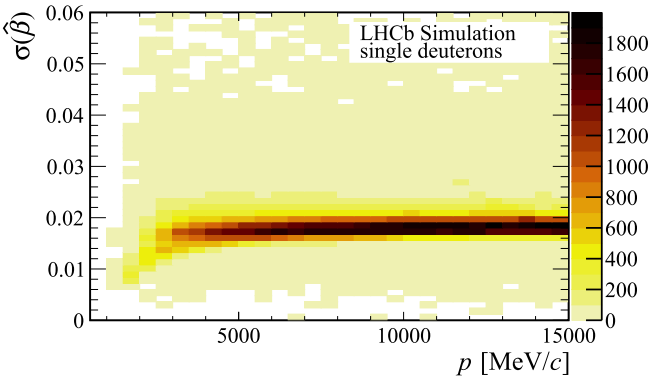

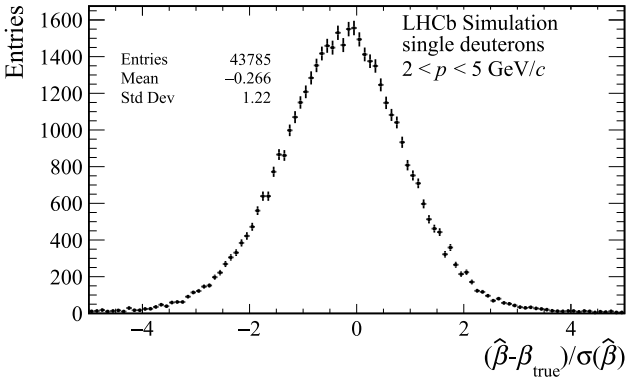

Fig. 4 Performance of the β determination on the simulated sample of single deuteron tracks: (left) estimated uncertainty $\sigma(\hat{\beta})$ as a function of momentum; (right) normalised residuals for low-momentum particles

Track fits with different values of β are performed with a fixed number of detector hits, starting from those associated to the track by the TofForward algorithm. The drift-time information is always used, even when the reconstructed value is apparently above its physically allowed maximum value of 35 ns. These two prescriptions are needed to obtain a well-behaved β dependence of χ^2_β, with a profile that approximates a parabola in the region surrounding the minimum. To speed up the algorithm, the minimum of χ^2_β is found with a gradient descent algorithm, starting from $\beta = 1$ and a negative step of 0.01. The sampled β values are limited between 1.1 and the value corresponding to a mass of 4 GeV/c^2 for the measured particle momentum. The values around the minimum are fitted with a second-order polynomial to obtain the estimated value $\hat{\beta}$ and its uncertainty $\sigma(\hat{\beta})$. To reduce biases from hits that are incorrectly assigned to the track, the $\hat{\beta}$ determination is updated if some hits in the track fit for $\beta = \hat{\beta}$ exhibit a residual larger than three standard deviations. The procedure is repeated up to four times, removing up to two outlier hits on every iteration.

Figure 4 shows the performance for simulated single deuterons: $\sigma(\hat{\beta})$ is typically below 0.02 for $p < 3$ GeV/c ($\beta < 0.73$) and the bias on the β determination, defined as the difference between the estimated value $\hat{\beta}$ and the true value β_{true}, is well below its average uncertainty. Results for the β measurements on different hadron species in the PYTHIA-based simulation are shown in Fig. 5.

While the simulated collision samples are enriched with deuterons, the antideuteron/antiproton production ratio for $p < 5$ GeV/c in fixed-target collisions at the LHCb experiment is expected to be between 10^{-4} and 10^{-3} [23]. The isolation of a deuteron sample requires more discriminating power against lighter hadrons than the one achievable with the $\hat{\beta}$ estimator alone. This is illustrated in Fig. 6, showing the distribution of the estimated particle mass from the time-of-flight and momentum measurements

$$\hat{\text{M}}_{\text{TOF}} \equiv \frac{p}{c}\sqrt{\frac{1}{\min(\hat{\beta},1)^2}-1}\,, \tag{2}$$

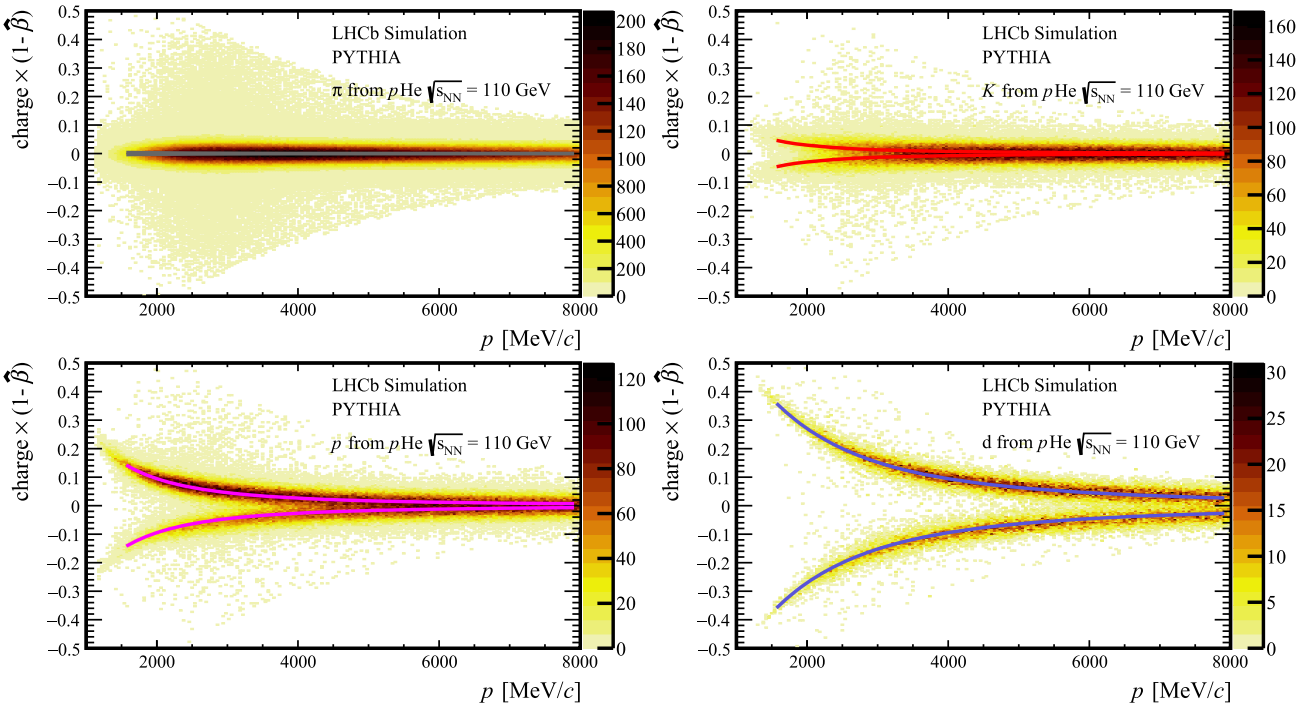

Fig. 5 Difference with respect to 1 of $\hat{\beta}$, multiplied by the particle charge, as a function of the reconstructed momentum for four hadron species in the PYTHIA-based simulated sample: (top left) pions, (top right) kaons, (bottom left) protons and (bottom right) deuterons. The overlaid curves show the expected relations

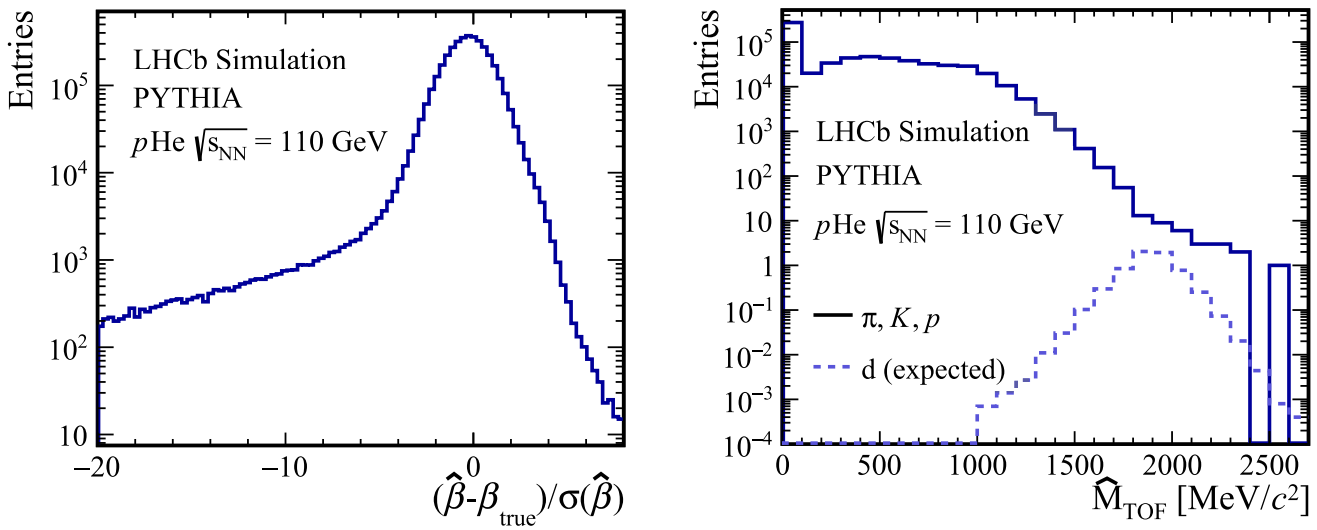

Fig. 6 (Left) Residual of the β estimation normalised by its estimated uncertainty for simulated positively charged particles with momentum below 4 GeV/c. (Right) Distribution of the corresponding estimated mass $\hat{M}_{\mathrm{TOF}}$, separately for deuterons and lighter particles, assuming that a deuteron is produced approximately one out of every 10^4 collisions

for the expected deuteron signal and for lighter particles. A significant background to deuteron identification is expected from cases where β is underestimated by an amount far beyond its estimated uncertainty.

This background is studied in simulation by selecting those hadrons among pions, kaons, and protons whose $\hat{M}_{\mathrm{TOF}}$ value is compatible with the deuteron mass within 400 MeV/c^2, called fake deuterons in the following. Several

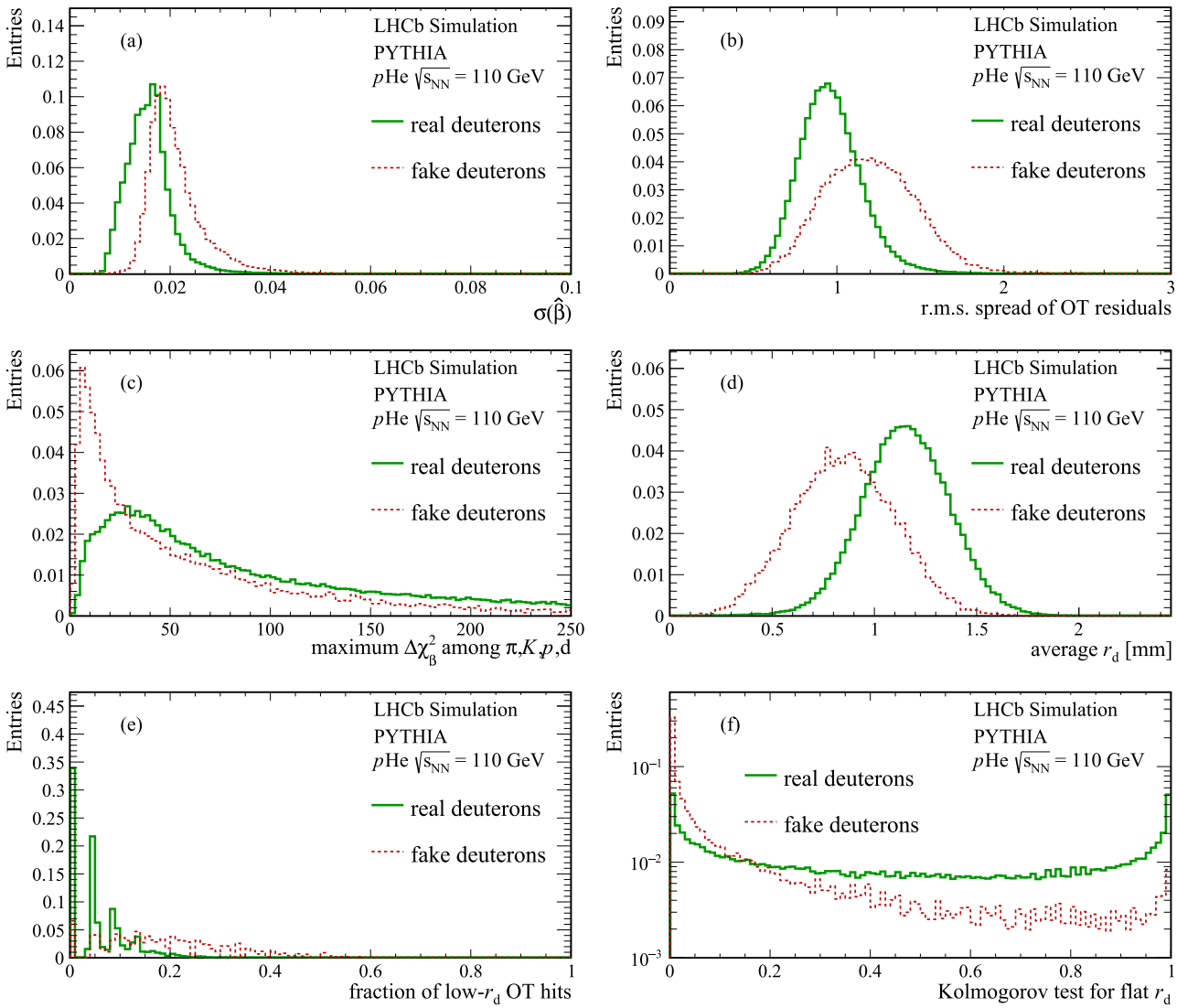

Fig. 7 Distributions in simulation of some of the observables used to discriminate genuine deuterons from lighter particles with an $\hat{M}_{TOF}$ value compatible with the deuteron mass (fake deuterons), for tracks with momentum lower than 3 GeV/c

observables related to the quality of the track fit and β determination are considered in order to identify fake deuterons and improve the β estimation. Observables that are found to provide significant discrimination between fake and real deuterons of equal momentum include the uncertainty $\sigma(\hat{\beta})$, shown in Fig. 7a, the number of OT hits, the quality of the reconstructed track (track χ^2, average and spread of residuals in the OT as in Fig. 7b, variation of the track χ^2 and of the number of outliers between the track fits with $\beta = 1$ and $\beta = \hat{\beta}$), the maximum difference in χ^2_β among four hadron hypotheses (π, K, p, d) in Fig. 7c, and the distribution of the reconstructed drift radius r_d in the OT straw tubes, namely the distance from the straw tube wire corresponding to the reconstructed drift time. The r_d observable is particularly important since for light hadrons with underestimated β, the reconstructed drift times are underestimated, while a flat distribution of the drift radius between 0 and its maximum value of 2.5 mm is expected for properly reconstructed tracks. This is exploited by computing four observables from the OT hits associated to each track candidate: the average and r.m.s. spread of drift radii in Fig. 7d, the fraction of r_d values lower than 0.2 mm in the distribution of Fig. 7e and the result of a Kolmogorov–Smirnov test [24] of the r_d values against a uniform distribution between 0 and 2.5 mm in Fig. 7f.

A total of 13 variables, including the particle momentum, are fed into an artificial neural network (ANN), trained on simulated collisions to predict the residual $\Delta\beta = \hat{\beta} - \beta_{true}$, where β_{true} is the true value from simulation. To avoid that any requirement on the network output could bias the particle identification by producing fake peaks in the $\hat{M}_{TOF}$ distribu-

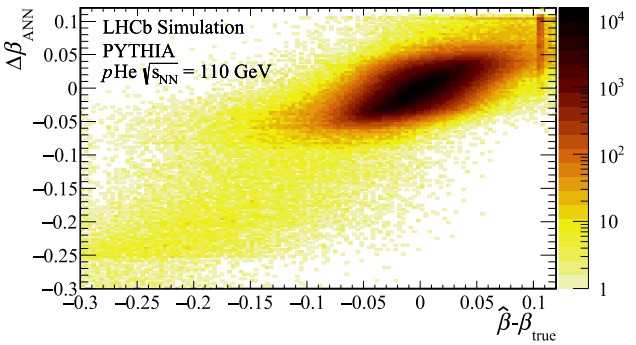

Fig. 8 Performance of the $\Delta\beta_{\text{ANN}}$ predictor on simulated collisions. The response is shown for all track candidates with momentum lower than 5 GeV/c. The structure at $\Delta\beta = 0.1$ is an artifact from the limit $\beta < 1.1$ on the sampled values

tion, no input is provided about the particle type and its true or measured speed. The goal is to obtain an assessment of the accuracy of the β estimation from observables related to the quality of the fit without prior knowledge of the estimated β value.

The network, implemented using KERAS [25] with TENSORFLOW [26] backend, consists of two tanh-activated hidden layers with 32 neurons each and is trained on 60% of the simulated collision sample. The performance of the resulting predictor $\Delta\beta_{\text{ANN}}$ is illustrated in Fig. 8 in the remaining 40% of simulated collisions. The results show that the predictor identifies most of the cases where β is badly underestimated, so that fake deuterons can be suppressed by requiring a small value of $|\Delta\beta_{\text{ANN}}|$. Moreover, it shows a good correlation with the actual residual even in the bulk of the distribution, allowing the β estimator to be refined as

$$\hat{\beta}_{\text{ANN}} \equiv \hat{\beta} - \Delta\beta_{\text{ANN}}. \tag{3}$$

The resulting improvement of the β estimation is illustrated in Fig. 9.

4 Performance

The performance obtained in simulation is verified on a sample of pHe collisions at $\sqrt{s_{\text{NN}}}$ =110 GeV, collected in 2016 with loose online selection requirements. The sample consists of about 700 million events, corresponding to an integrated luminosity of 0.5 nb^{-1} [27].

The β determination procedure is first verified on identified pion and proton tracks from $K^0_S \to \pi^+\pi^-$ and $\Lambda \to p\pi^-$ decays, for which the identity of the particles can be determined from the decay kinematics [28]. Candidates are selected based on their incompatibility with originating from the primary collision vertex, the reconstructed mass of the decaying resonance, and the quality of the reconstructed decay vertex. The purity of these calibration samples exceeds 98%. The same exercise is performed on the simulated sample and the distributions of the observables used in this study

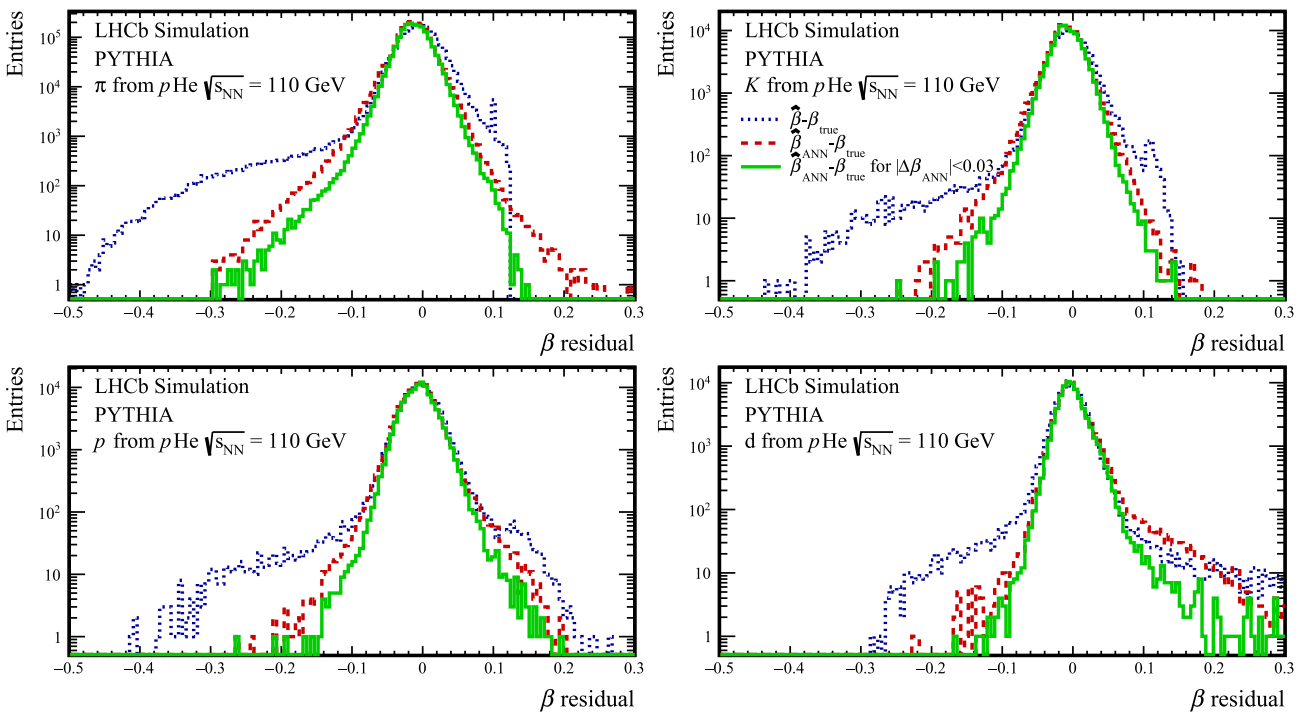

Fig. 9 Impact of the use of the $\Delta\beta_{\text{ANN}}$ predictor on the accuracy of the β determination for different hadron species in simulated collisions, for tracks with momentum lower than 5 GeV/c

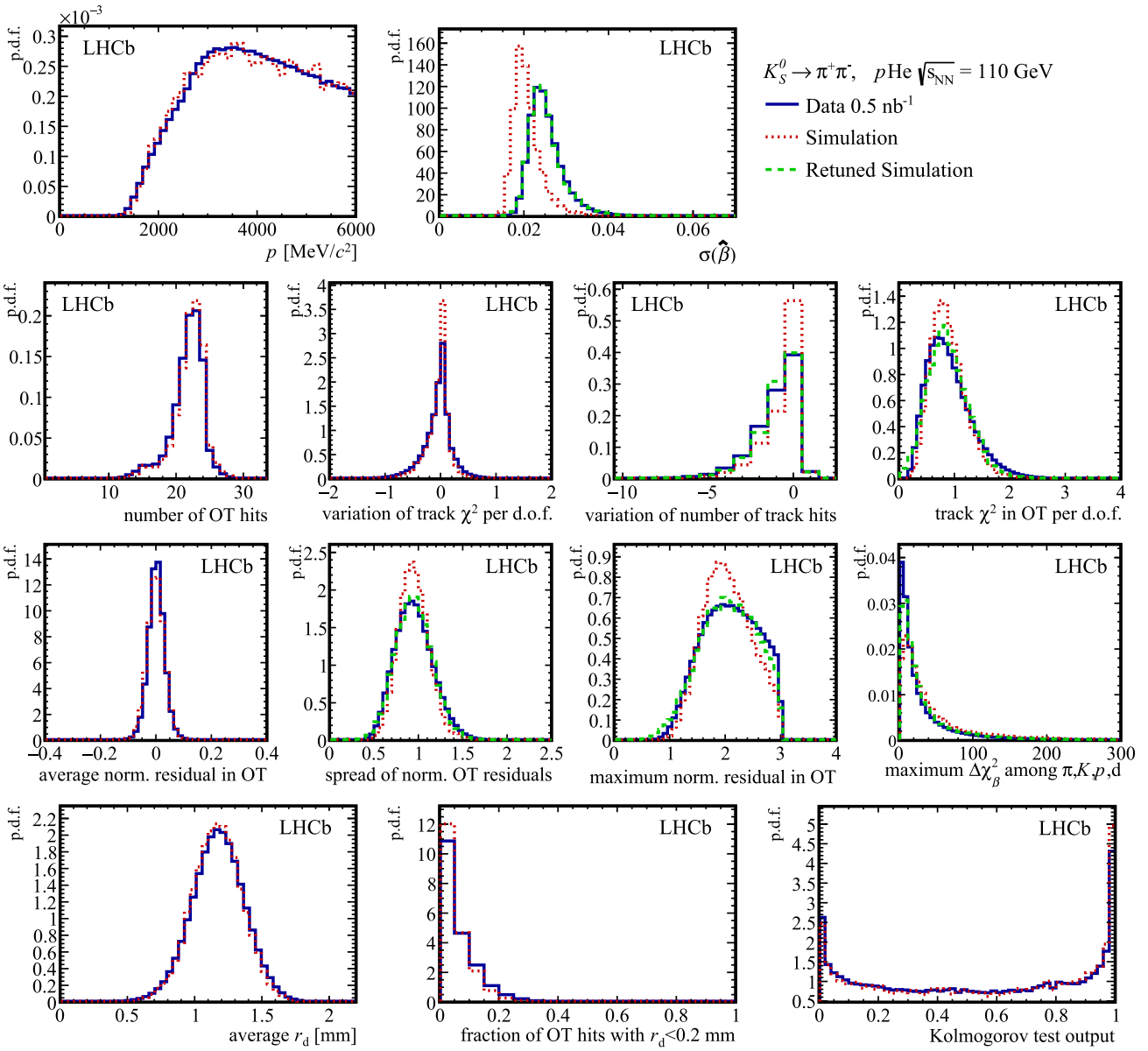

Fig. 10 Distributions of the 13 observables, described in Sec. 3, used as input to the $\Delta\beta_{\text{ANN}}$ predictor network. Data and simulation are compared for candidate pion tracks from K^0_S decays with momentum below 6 GeV/c. For six variables, notably $\sigma(\hat{\beta})$, an empirical correction is applied to the simulated observables to improve the agreement with data

are shown in Fig. 10 to be in a good overall agreement with data. The largest difference that can be noticed is a larger average value of $\sigma(\hat{\beta})$ in data. Comparing the $\hat{\beta}$ estimation with the expected β from the measured momentum and the known mass of the identified pion or proton, a negative bias is seen, of order 0.01 and larger than the one observed in simulation. Both effects, the differences in $\hat{\beta}$ and $\sigma(\hat{\beta})$ values, are compatible with a residual miscalibration of the OT response of $\mathcal{O}(0.1)$ ns. The bias on $\hat{\beta}$ is corrected by parametrising it with an empirical function of p and $\hat{\beta}$ tuned on the calibration sample.

Two $\Delta\beta_{\text{ANN}}$ predictor networks are retrained making use of the calibration data. The first is directly trained on the calibration tracks, using 80% of the sample. The second network is trained on the simulated collisions after correcting for the observed differences in the distribution of $\sigma(\hat{\beta})$ and other five input variables, as shown in Fig. 10. The $\sigma(\hat{\beta})$ value is scaled by a factor $(1 + k\hat{\beta}^2)$, where $k = 0.22$ is obtained from the calibration pion sample and the β dependence from a miscalibration effect is assumed. For the other variables, the correction consists of adding a Gaussian-smeared value to reproduce the average and r.m.s. spread of the distribution observed in the calibration data.

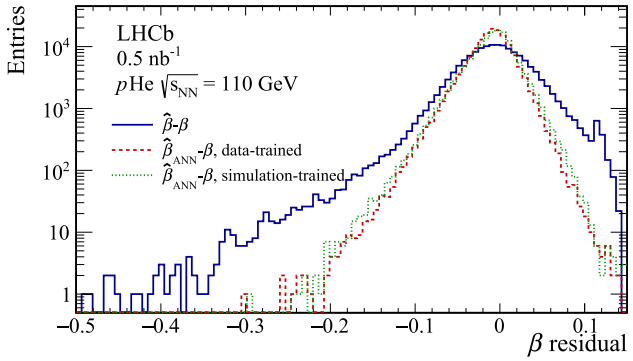

Fig. 11 Performance of the $\Delta\beta_{\mathrm{ANN}}$ predictor on the calibration sample, for momenta lower than 5 GeV/c. The plot shows the difference between the β estimation and the expected value $\beta = p/\sqrt{[p^2 + (Mc)^2]}$, obtained from the measured momentum and the known mass M of the identified pion or proton. The comparison is performed on the 20% of calibration data not used for the training

Figure 11 presents a comparison of the performance of the two networks on the 20% of the calibration data that was not used during training. Though the data-driven predictor has slightly better performance, the network trained on simulation identifies correctly most of the fake deuterons in the calibration sample and is preferred in the following to avoid any overtraining in data. Moreover, its training includes deuterons, which are the main goal of this study and for which no data calibration sample is available.

The β determination is finally performed on the whole sample of reconstructed low-momentum tracks ($p < 6$ GeV/c) with loose preselection requirements (at least 6 OT hits and $\sigma(\hat{\beta}) < 0.1$). Figure 12 shows the reconstructed mass values in different momentum intervals for positively charged particles, using the $\hat{\beta}$ or $\hat{\beta}_{\mathrm{ANN}}$ estimators and with or without an additional requirement on the $\Delta\beta_{\mathrm{ANN}}$ predictor. A clear deuteron signal is visible for $p < 2.5$ GeV/c, and an excess of tracks in the region of the triton mass is also observed. These ion candidates are expected to be mostly produced by the fragmentation of the helium target and are clearly visible only in the sample with reconstructed tracks of positively charged particles.

As expected from the studies on simulation, the neural-network-based predictor $\hat{\beta}_{\mathrm{ANN}}$ provides better discrimination among particle species than $\hat{\beta}$, and the deuteron identification is further improved by the $\Delta\beta_{\mathrm{ANN}}$ requirement. The distribution of $\hat{\beta}_{\mathrm{ANN}}$ as a function of momentum for tracks of positively charged particles with $|\Delta\beta_{\mathrm{ANN}}| < 0.03$ is shown in Fig. 13.

A few He ion candidates are also identified in the pHe sample, thanks to their ionisation losses in the Si-based tracking detectors [8]. The OT timing response for particles with atomic number $Z = 2$ (or larger) is biased toward shorter drift

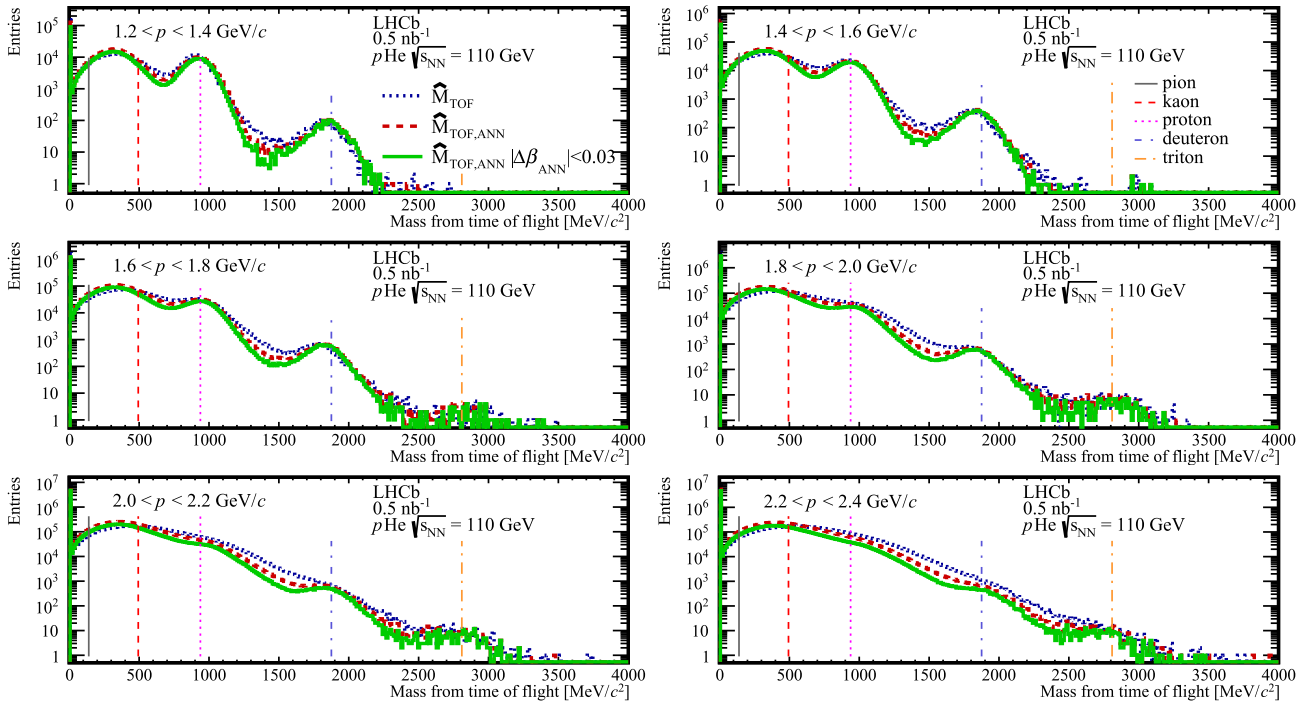

Fig. 12 Estimated particle mass from the time of flight for reconstructed tracks of positively charged particles in the pHe collision sample, for different momentum intervals. $\hat{M}_{\mathrm{TOF,ANN}}$ is obtained by replacing $\hat{\beta}$ with $\hat{\beta}_{\mathrm{ANN}}$ in Eq. 2. The vertical lines correspond to the known mass of pions, kaons, protons, deuterons and tritons

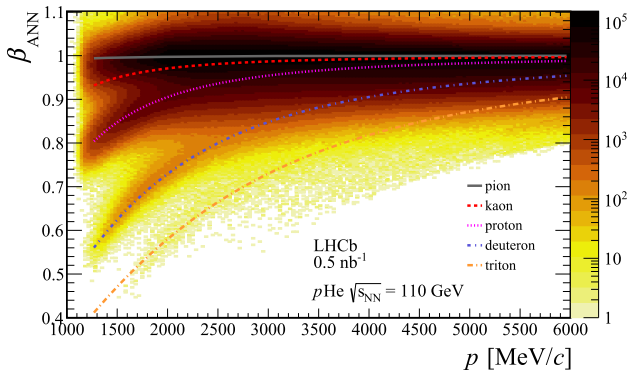

Fig. 13 Estimated speed versus momentum for reconstructed tracks of positively charged particles in the pHe collision sample, using the $\hat{\beta}_{\text{ANN}}$ estimator and requiring $|\Delta\beta_{\text{ANN}}| < 0.03$. The overlaid curves show the expected relations for different hadron species. Proton, deuteron and triton production can be seen. The momentum-dependent cutoff at low β corresponds to the maximum mass hypothesis allowed in the algorithm

times, due to their higher ionisation with respect to $Z = 1$ particles. In the explored low-momentum region, the biased reconstructed speed roughly corresponds to that expected for protons. Therefore, the time-of-flight technique is not suitable by itself to discriminate low-momentum He nuclei from lighter particles, though it could provide some discrimination between ^{3}He and ^{4}He candidates. For He nuclei with momentum larger than 10 GeV/c, the measured time of flight in the OT is apparently shorter than that expected for $\beta = 1$, a feature that is already exploited in the He identification tool described in Ref. [8].

5 Conclusions

In this paper, a newly developed identification tool for light ions is presented, exploiting the available timing information of the LHCb detector operated in the LHC Run 2 to distinguish low-momentum deuterons from lighter hadrons by their time of flight. The tool performance is demonstrated by showing its capability to identify a signal for deuteron and triton production in pHe collisions at $\sqrt{s_{\text{NN}}}$ =110 GeV.

The benchmark sample has been chosen as it reproduces collisions of cosmic rays on the interstellar medium at the energy scale corresponding to the capabilities of the AMS-02 spectrometer. Though this time-of-flight technique in the LHCb detector can be exploited only in a limited kinematic region, it opens the way to unique and much awaited measurements of light antinuclei production at this energy scale, constraining the expected flux of secondary cosmic antideuterons.

Acknowledgements We express our gratitude to our colleagues in the CERN accelerator departments for the excellent performance of the LHC. We thank the technical and administrative staff at the LHCb institutes. We acknowledge support from CERN and from the national agencies: ARC (Australia); CAPES, CNPq, FAPERJ and FINEP (Brazil); MOST and NSFC (China); CNRS/IN2P3 (France); BMBF, DFG and MPG (Germany); INFN (Italy); NWO (Netherlands); MNiSW and NCN (Poland); MCID/IFA (Romania); MICIU and AEI (Spain); SNSF and SER (Switzerland); NASU (Ukraine); STFC (United Kingdom); DOE NP and NSF (USA). We acknowledge the computing resources that are provided by ARDC (Australia), CBPF (Brazil), CERN, IHEP and LZU (China), IN2P3 (France), KIT and DESY (Germany), INFN (Italy), SURF (Netherlands), Polish WLCG (Poland), IFIN-HH (Romania), PIC (Spain), CSCS (Switzerland), and GridPP (United Kingdom). We are indebted to the communities behind the multiple open-source software packages on which we depend. Individual groups or members have received support from Key Research Program of Frontier Sciences of CAS, CAS PIFI, CAS CCEPP, Fundamental Research Funds for the Central Universities, and Sci. and Tech. Program of Guangzhou (China); Minciencias (Colombia); EPLANET, Marie Skłodowska-Curie Actions, ERC and NextGenerationEU (European Union); A*MIDEX, ANR, IPhU and Labex P2IO, and Région Auvergne-Rhône-Alpes (France); Alexander-von-Humboldt Foundation (Germany); ICSC (Italy); Severo Ochoa and María de Maeztu Units of Excellence, GVA, XuntaGal, GENCAT, InTalent-Inditex and Prog. Atracción Talento CM (Spain); SRC (Sweden); the Leverhulme Trust, the Royal Society and UKRI (United Kingdom).

Data Availability Statement This manuscript has associated data in a data repository. [Author's comment: The datasets generated during and/or analysed during the current study are available at https://cds.cern.ch/record/2940031.]

Code Availability Statement Code/software will be made available on reasonable request. [Author's comment: The code/software generated during and/or analysed during the current study is available from the corresponding author on reasonable request.]

Funded by SCOAP^3.

References

1. P. Salati, F. Donato, N. Fornengo, *Indirect Dark Matter Detection with Cosmic Antimatter*, arXiv:1003.4124
2. AMS collaboration, M. Aguilar et al., *The Alpha Magnetic Spectrometer (AMS) on the international space station: Part II – Results from the first seven years*, Phys. Rept. **894** (2021) 1 https://doi.org/10.1016/j.physrep.2020.09.003
3. S. Ting, Latest results from AMS on the International Space Station, 8 June 2023. https://indico.cern.ch/event/1275785/
4. LHCb collaboration, A. A. Alves Jr. *et al.*, The LHCb detector at the LHC, JINST **3** (2008) S08005 https://doi.org/10.1088/1748-0221/3/08/S08005
5. LHCb collaboration, R. Aaij et al., LHCb detector performance, Int. J. Mod. Phys. **A30** (2015) 1530022, arXiv:1412.6352. https://doi.org/10.1142/S0217751X15300227

6. C. Barschel, Precision luminosity measurement at LHCb with beam-gas imaging, PhD thesis, RWTH Aachen U., 2014, CERN-THESIS-2013-301. https://cds.cern.ch/record/1693671
7. A. Bursche et al., *Physics opportunities with the fixed-target program of the LHCb experiment using an unpolarized gas target*, , CERN-LHCb-PUB-2018-015. https://cds.cern.ch/record/2649878
8. LHCb collaboration, R. Aaij et al., Helium identification with LHCb, JINST **19** (2024) P02010, arXiv:2310.05864. https://doi.org/10.1088/1748-0221/19/02/P02010
9. S. K. Baker, Measurement of deuterons at LHCb, PhD thesis, Imperial Coll., London, 2019, https://doi.org/10.25560/97672
10. LHCb collaboration, *LHCb outer tracker: Technical Design Report*, CERN-LHCC-2001-024, 2001 http://cdsweb.cern.ch/search?p=CERN-LHCC-2001-024&f=reportnumber&action_search=Search&c=LHCb
11. P. d'Argent et al., Improved performance of the lhcb outer tracker in lhc run 2. JINST **12**, P11016 (2017). https://doi.org/10.1088/1748-0221/12/11/P11016. arXiv:1708.00819
12. A.A. Alves Jr. et al., Performance of the lhcb muon system. JINST **8**, P02022 (2013). https://doi.org/10.1088/1748-0221/8/02/P02022. arXiv:1211.1346
13. M. De Cian, Track reconstruction efficiency and analysis of $B^0 \to K^{*0}\mu^+\mu^-$ at the LHCb experiment, PhD thesis, Zurich University, 2013, https://cds.cern.ch/record/1605179
14. O. Callot, S. Hansmann-Menzemer, The forward tracking: Algorithm and performance studies, LHCb-2007-015, CERN-LHCb-2007-015, CERN, Geneva, (2007). https://cds.cern.ch/record/1033584
15. S. Ostapchenko, Monte carlo treatment of hadronic interactions in enhanced pomeron scheme: qgsjet-ii model. Phys. Rev. D **83**, 014018 (2011). https://doi.org/10.1103/PhysRevD.83.014018. arXiv:1010.1869
16. T. Sjöstrand, S. Mrenna, P. Skands, PYTHIA 6.4 physics and manual, JHEP **05** (2006) 026, arXiv:hep-ph/0603175. https://doi.org/10.1088/1126-6708/2006/05/026
17. ALICE collaboration, Supplemental material: afterburner for generating light (anti-)nuclei with QCD-inspired event generators in pp collisions, , ALICE-PUBLIC-2017-010. https://cds.cern.ch/record/2285500
18. Geant4 collaboration, J. Allison et al., Geant4 developments and applications, IEEE Trans. Nucl. Sci. **53** (2006) 270. https://doi.org/10.1109/TNS.2006.869826
19. Geant4 collaboration, S. Agostinelli *et al.*, *Geant4: A simulation toolkit*, Nucl. Instrum. Meth. **A506** (2003) 250. https://doi.org/10.1016/S0168-9002(03)01368-8
20. M. Clemencic et al., The lhcb simulation application, gauss: design, evolution and experience. J. Phys: Conf. Ser. **331**, 032023 (2011). https://doi.org/10.1088/1742-6596/331/3/032023
21. LHCb collaboration, M. Stahl, Machine learning and parallelism in the reconstruction of LHCb and its upgrade, J. Phys. Conf. Ser. **898** (2017) 042042, arXiv:1710.08947. https://doi.org/10.1088/1742-6596/898/4/042042
22. R. Aaij et al., Design and performance of the lhcb trigger and full real-time reconstruction in run 2 of the lhc. JINST **14**, P04013 (2019). https://doi.org/10.1088/1748-0221/14/04/P04013. arXiv:1812.10790
23. C. Lucarelli, Extending the physics reach of the fixed-target programme at the LHCb experiment, PhD thesis, Florence University, (2024), https://cds.cern.ch/record/2889345
24. N. Smirnov, Table for estimating the goodness of fit of empirical distributions. Ann. Math. Stat. **19**, 279 (1948). https://doi.org/10.1214/aoms/1177730256
25. F. Chollet et al., Keras, https://keras.io, (2015)
26. M. Abadi et al., TensorFlow: Large-scale machine learning on heterogeneous systems, https://www.tensorflow.org/, (2015)
27. LHCb collaboration, R. Aaij et al., Measurement of antiproton production in pHe collisions at $\sqrt{s_{\rm NN}} = 110$ GeV, Phys. Rev. Lett. **121** (2018) 222001, arXiv:1808.06127. https://doi.org/10.1103/PhysRevLett.121.222001
28. J. Podolanski, R. Armenteros, Analysis of v-events. Philos. Mag. **45**, 13 (1954). https://doi.org/10.1080/14786440108520416

LHCb Collaboration

R. Aaij[38], A. S. W. Abdelmotteleb[57], C. Abellan Beteta[51], F. Abudinén[57], T. Ackernley[61], A. A. Adefisoye[69], B. Adeva[47], M. Adinolfi[55], P. Adlarson[85], C. Agapopoulou[14], C. A. Aidala[87], Z. Ajaltouni[11], S. Akar[11], K. Akiba[38], M. Akthar[40], P. Albicocco[28], J. Albrecht[19,g], R. Aleksiejunas[80], F. Alessio[49], P. Alvarez Cartelle[56], R. Amalric[16], S. Amato[3], J. L. Amey[55], Y. Amhis[14], L. An[6], L. Anderlini[27], M. Andersson[51], P. Andreola[51], M. Andreotti[26], S. Andres Estrada[84], A. Anelli[31,49,p], D. Ao[7], C. Arata[12], F. Archilli[37,w], Z Areg[69], M. Argenton[26], S. Arguedas Cuendis[9,49], L. Arnone[31,p], A. Artamonov[44], M. Artuso[69], E. Aslanides[13], R. Ataíde Da Silva[50], M. Atzeni[65], B. Audurier[12], J. A. Authier[15], D. Bacher[64], I. Bachiller Perea[50], S. Bachmann[22], M. Bachmayer[50], J. J. Back[57], P. Baladron Rodriguez[47], V. Balagura[15], A. Balboni[26], W. Baldini[26], Z. Baldwin[78], L. Balzani[19], H. Bao[7], J. Baptista de Souza Leite[2], C. Barbero Pretel[12,47], M. Barbetti[27], I. R. Barbosa[70], R. J. Barlow[63], M. Barnyakov[25], S. Barsuk[14], W. Barter[59], J. Bartz[69], S. Bashir[40], B. Batsukh[5], P. B. Battista[14], A. Bay[50], A. Beck[65], M. Becker[19], F. Bedeschi[35], I. B. Bediaga[2], N. A. Behling[19], S. Belin[47], A. Bellavista[25], K. Belous[44], I. Belov[29], I. Belyaev[36], G. Benane[13], G. Bencivenni[28], E. Ben-Haim[16], A. Berezhnoy[44], R. Bernet[51], S. Bernet Andres[46], A. Bertolin[33], F. Betti[59], J. Bex[56], O. Bezshyyko[86], J. Bhom[41], M. S. Bieker[18], N. V. Biesuz[26], A. Biolchini[38], M. Birch[62], F. C. R. Bishop[10], A. Bitadze[63], A. Bizzeti[27,q], T. Blake[57,c], F. Blanc[50], J. E. Blank[19], S. Blusk[69], V. Bocharnikov[44], J. A. Boelhauve[19], O. Boente Garcia[15], T. Boettcher[68], A. Bohare[59], A. Boldyrev[44], C. S. Bolognani[82], R. Bolzonella[26,m],

R. B. Bonacci[1], N. Bondar[44,49], A. Bordelius[49], F. Borgato[33,49], S. Borghi[63], M. Borsato[31,p], J. T. Borsuk[83], E. Bottalico[61], S. A. Bouchiba[50], M. Bovill[64], T. J. V. Bowcock[61], A. Boyer[49], C. Bozzi[26], J. D. Brandenburg[88], A. Brea Rodriguez[50], N. Breer[19], J. Brodzicka[41], A. Brossa Gonzalo[47,*], J. Brown[61], D. Brundu[32], E. Buchanan[59], M. Burgos Marcos[82], A. T. Burke[63], C. Burr[49], C. Buti[27], J. S. Butter[56], J. Buytaert[49], W. Byczynski[49], S. Cadeddu[32], H. Cai[75], Y. Cai[5], A. Caillet[16], R. Calabrese[26,m], S. Calderon Ramirez[9], L. Calefice[45], M. Calvi[31,p], M. Calvo Gomez[46], P. Camargo Magalhaes[2,a], J. I. Cambon Bouzas[47], P. Campana[28], D. H. Campora Perez[82], A. F. Campoverde Quezada[7], S. Capelli[31], M. Caporale[25], L. Capriotti[26], R. Caravaca-Mora[9], A. Carbone[25,k], L. Carcedo Salgado[47], R. Cardinale[29,n], A. Cardini[32], P. Carniti[31], L. Carus[22], A. Casais Vidal[65], R. Caspary[22], G. Casse[61], M. Cattaneo[49], G. Cavallero[26], V. Cavallini[26,m], S. Celani[22], I. Celestino[35,t], S. Cesare[30,o], F. Cesario Laterza Lopes[2], A. J. Chadwick[61], I. Chahrour[87], H. Chang[4,d], M. Charles[16], Ph. Charpentier[49], E. Chatzianagnostou[38], R. Cheaib[79], M. Chefdeville[10], C. Chen[56], J. Chen[50], S. Chen[5], Z. Chen[7], M. Cherif[12], A. Chernov[41], S. Chernyshenko[53], X. Chiotopoulos[82], V. Chobanova[84], M. Chrzaszcz[41], A. Chubykin[44], V. Chulikov[28,36,49], P. Ciambrone[28], X. Cid Vidal[47], G. Ciezarek[49], P. Cifra[38], P. E. L. Clarke[59], M. Clemencic[49], H. V. Cliff[56], J. Closier[49], C. Cocha Toapaxi[22], V. Coco[49], J. Cogan[13], E. Cogneras[11], L. Cojocariu[43], S. Collaviti[50], P. Collins[49], T. Colombo[49], M. Colonna[19], A. Comerma-Montells[45], L. Congedo[24], J. Connaughton[57], A. Contu[32], N. Cooke[60], G. Cordova[35,t], C. Coronel[66], I. Corredoira[12], A. Correia[16], G. Corti[49], J. Cottee Meldrum[55], B. Couturier[49], D. C. Craik[51], M. Cruz Torres[2,h], E. Curras Rivera[50], R. Currie[59], C. L. Da Silva[68], S. Dadabaev[44], L. Dai[72], X. Dai[4], E. Dall'Occo[49], J. Dalseno[84], C. D'Ambrosio[62], J. Daniel[11], P. d'Argent[24], G. Darze[3], A. Davidson[57], J. E. Davies[63], O. De Aguiar Francisco[63], C. De Angelis[32,l], F. De Benedetti[49], J. de Boer[38], K. De Bruyn[81], S. De Capua[63], M. De Cian[63], U. De Freitas Carneiro Da Graca[2,b], E. De Lucia[28], J. M. De Miranda[2], L. De Paula[3], M. De Serio[24,i], P. De Simone[28], F. De Vellis[19], J. A. de Vries[82], F. Debernardis[24], D. Decamp[10], S. Dekkers[1], L. Del Buono[16], B. Delaney[65], H.-P. Dembinski[19], J. Deng[8], V. Denysenko[51], O. Deschamps[11], F. Dettori[32,l], B. Dey[79], P. Di Nezza[28], I. Diachkov[44], S. Didenko[44], S. Ding[69], Y. Ding[50], L. Dittmann[22], V. Dobishuk[53], A. D. Docheva[60], A. Doheny[57], C. Dong[4,d], A. M. Donohoe[23], F. Dordei[32], A. C. dos Reis[2], A. D. Dowling[69], L. Dreyfus[13], W. Duan[73], P. Duda[83], L. Dufour[49], V. Duk[34], P. Durante[49], M. M. Duras[83], J. M. Durham[68], O. D. Durmus[79], A. Dziurda[41], A. Dzyuba[44], S. Easo[58], E. Eckstein[18], U. Egede[1], A. Egorychev[44], V. Egorychev[44], S. Eisenhardt[59], E. Ejopu[61], L. Eklund[85], M. Elashri[66], J. Ellbracht[19], S. Ely[62], A. Ene[43], J. Eschle[69], S. Esen[22], T. Evans[38], F. Fabiano[32], S. Faghih[66], L. N. Falcao[2], B. Fang[7], R. Fantechi[35], L. Fantini[34,s], M. Faria[50], K. Farmer[59], D. Fazzini[31,p], L. Felkowski[83], M. Feng[5,7], M. Feo[19], A. Fernandez Casani[48], M. Fernandez Gomez[47], A. D. Fernez[67], F. Ferrari[25,k], F. Ferreira Rodrigues[3], M. Ferrillo[51], M. Ferro-Luzzi[49], S. Filippov[44], R. A. Fini[24], M. Fiorini[26,m], M. Firlej[40], K. L. Fischer[64], D. S. Fitzgerald[87], C. Fitzpatrick[63], T. Fiutowski[40], F. Fleuret[15], A. Fomin[52], M. Fontana[25], L. F. Foreman[63], R. Forty[49], D. Foulds-Holt[59], V. Franco Lima[3], M. Franco Sevilla[67], M. Frank[49], E. Franzoso[26,m], G. Frau[63], C. Frei[49], D. A. Friday[49,63], J. Fu[7], Q. Führing[19,56,g], T. Fulghesu[13], G. Galati[24], M. D. Galati[38], A. Gallas Torreira[47], D. Galli[25,k], S. Gambetta[59], M. Gandelman[3], P. Gandini[30], B. Ganie[63], H. Gao[7], R. Gao[64], T. Q. Gao[56], Y. Gao[8], Y. Gao[6], Y. Gao[8], L. M. Garcia Martin[50], P. Garcia Moreno[45], J. García Pardiñas[65], P. Gardner[67], K. G. Garg[8], L. Garrido[45], C. Gaspar[49], A. Gavrikov[33], L. L. Gerken[19], E. Gersabeck[20], M. Gersabeck[20], T. Gershon[57], S. Ghizzo[29,n], Z. Ghorbanimoghaddam[55], F. I. Giasemis[16,f], V. Gibson[56], H. K. Giemza[42], A. L. Gilman[66], M. Giovannetti[28], A. Gioventù[45], L. Girardey[58,63], M. A. Giza[41], F. C. Glaser[14,22], V. V. Gligorov[16], C. Göbel[70], L. Golinka-Bezshyyko[86], E. Golobardes[46], D. Golubkov[44], A. Golutvin[49,62], S. Gomez Fernandez[45], W. Gomulka[40], I. Gonçales Vaz[49], F. Goncalves Abrantes[64], M. Goncerz[41], G. Gong[4,d], J. A. Gooding[19], I. V. Gorelov[44], C. Gotti[31], E. Govorkova[65], J. P. Grabowski[30], L. A. Granado Cardoso[49], E. Graugés[45], E. Graverini[50,u], L. Grazette[57], G. Graziani[27], A. T. Grecu[43], N. A. Grieser[66], L. Grillo[60], S. Gromov[44], C. Gu[15], M. Guarise[26], L. Guerry[11], V. Guliaeva[44], P. A. Günther[22], A.-K. Guseinov[50], E. Gushchin[44], Y. Guz[6,49], T. Gys[49], K. Habermann[18], T. Hadavizadeh[1], C. Hadjivasiliou[67], G. Haefeli[50], C. Haen[49], S. Haken[56], G. Hallett[57], P. M. Hamilton[67], J. Hammerich[61], Q. Han[33], X. Han[22,49], S. Hansmann-Menzemer[22], L. Hao[7], N. Harnew[64], T. H. Harris[1], M. Hartmann[14], S. Hashmi[40], J. He[7,e], A. Hedes[63], F. Hemmer[49], C. Henderson[66], R. Henderson[14], R. D. L. Henderson[1], A. M. Hennequin[49], K. Hennessy[61], L. Henry[50], J. Herd[62], P. Herrero Gascon[22], J. Heuel[17], A. Heyn[13], A. Hicheur[3], G. Hijano Mendizabal[51], J. Horswill[63], R. Hou[8], Y. Hou[11], D. C. Houston[60], N. Howarth[61],

J. Hu[73], W. Hu[7], X. Hu[4,d], W. Hulsbergen[38], R. J. Hunter[57], M. Hushchyn[44], D. Hutchcroft[61], M. Idzik[40], D. Ilin[44], P. Ilten[66], A. Iniukhin[44], A. Iohner[10], A. Ishteev[44], K. Ivshin[44], H. Jage[17], S. J. Jaimes Elles[77,48,49], S. Jakobsen[49], E. Jans[38], B. K. Jashal[48], A. Jawahery[67], C. Jayaweera[54], V. Jevtic[19], Z. Jia[16], E. Jiang[67], X. Jiang[5,7], Y. Jiang[7], Y. J. Jiang[6], E. Jimenez Moya[9], N. Jindal[88], M. John[64], A. John Rubesh Rajan[23], D. Johnson[54], C. R. Jones[56], S. Joshi[42], B. Jost[49], J. Juan Castella[56], N. Jurik[49], I. Juszczak[41], D. Kaminaris[50], S. Kandybei[52], M. Kane[59], Y. Kang[4,d], C. Kar[11], M. Karacson[49], A. Kauniskangas[50], J. W. Kautz[66], M. K. Kazanecki[41], F. Keizer[49], M. Kenzie[56], T. Ketel[38], B. Khanji[69], A. Kharisova[44], S. Kholodenko[62,49], G. Khreich[14], T. Kirn[17], V. S. Kirsebom[31,p], O. Kitouni[65], S. Klaver[39], N. Kleijne[35,t], D. K. Klekots[86], K. Klimaszewski[42], M. R. Kmiec[42], T. Knospe[19], R. Kolb[22], S. Koliiev[53], L. Kolk[19], A. Konoplyannikov[6], P. Kopciewicz[49], P. Koppenburg[38], A. Korchin[52], M. Korolev[44], I. Kostiuk[38], O. Kot[53], S. Kotriakhova, E. Kowalczyk[67], A. Kozachuk[44], P. Kravchenko[44], L. Kravchuk[44], O. Kravcov[80], M. Kreps[57], P. Krokovny[44], W. Krupa[69], W. Krzemien[42], O. Kshyvanskyi[53], S. Kubis[83], M. Kucharczyk[41], V. Kudryavtsev[44], E. Kulikova[44], A. Kupsc[85], V. Kushnir[52], B. Kutsenko[13], J. Kvapil[68], I. Kyryllin[52], D. Lacarrere[49], P. Laguarta Gonzalez[45], A. Lai[32], A. Lampis[32], D. Lancierini[62], C. Landesa Gomez[47], J. J. Lane[1], G. Lanfranchi[28], C. Langenbruch[22], J. Langer[19], O. Lantwin[44], T. Latham[57], F. Lazzari[35,49,u], C. Lazzeroni[54], R. Le Gac[13], H. Lee[61], R. Lefèvre[11], A. Leflat[44], S. Legotin[44], M. Lehuraux[57], E. Lemos Cid[49], O. Leroy[13], T. Lesiak[41], E. D. Lesser[49], B. Leverington[22], A. Li[4,d], C. Li[4,d], C. Li[13], H. Li[73], J. Li[8], K. Li[76], L. Li[63], M. Li[8], P. Li[7], P.-R. Li[74], Q. Li[5,7], T. Li[72], T. Li[73], Y. Li[8], Y. Li[5], Y. Li[4], Z. Lian[4,d], Q. Liang[8], X. Liang[69], Z. Liang[32], S. Libralon[48], A. L. Lightbody[12], C. Lin[7], T. Lin[58], R. Lindner[49], H. Linton[62], R. Litvinov[32], D. Liu[8], F. L. Liu[1], G. Liu[73], K. Liu[74], S. Liu[5,7], W. Liu[8], Y. Liu[59], Y. Liu[74], Y. L. Liu[62], G. Loachamin Ordonez[70], A. Lobo Salvia[45], A. Loi[32], T. Long[56], J. H. Lopes[3], A. Lopez Huertas[45], C. Lopez Iribarnegaray[47], S. López Soliño[47], Q. Lu[15], C. Lucarelli[49], D. Lucchesi[33,r], M. Lucio Martinez[48], Y. Luo[6], A. Lupato[33,j], E. Luppi[26,m], K. Lynch[23], X.-R. Lyu[7], G. M. Ma[4,d], H. Ma[72], S. Maccolini[19], F. Machefert[14], F. Maciuc[43], B. Mack[69], I. Mackay[64], L. M. Mackey[69], L. R. Madhan Mohan[56], M. J. Madurai[54], D. Magdalinski[38], D. Maisuzenko[44], J. J. Malczewski[41], S. Malde[64], L. Malentacca[49], A. Malinin[44], T. Maltsev[44], G. Manca[32,l], G. Mancinelli[13], C. Mancuso[14], R. Manera Escalero[45], F. M. Manganella[37], D. Manuzzi[25], D. Marangotto[30,o], J. F. Marchand[10], R. Marchevski[50], U. Marconi[25], E. Mariani[16], S. Mariani[49], C. Marin Benito[45], J. Marks[22], A. M. Marshall[55], L. Martel[64], G. Martelli[34], G. Martellotti[36], L. Martinazzoli[49], M. Martinelli[31,p], D. Martinez Gomez[81], D. Martinez Santos[84], F. Martinez Vidal[48], A. Martorell i Granollers[46], A. Massafferri[2], R. Matev[49], A. Mathad[49], V. Matiunin[44], C. Matteuzzi[69], K. R. Mattioli[15], A. Mauri[62], E. Maurice[15], J. Mauricio[45], P. Mayencourt[50], J. Mazorra de Cos[48], M. Mazurek[42], M. McCann[62], T. H. McGrath[63], N. T. McHugh[60], A. McNab[63], R. McNulty[23], B. Meadows[66], G. Meier[19], D. Melnychuk[42], D. Mendoza Granada[16], P. Menendez Valdes Perez[47], F. M. Meng[4,d], M. Merk[38,82], A. Merli[30,50], L. Meyer Garcia[67], D. Miao[5,7], H. Miao[7], M. Mikhasenko[78], D. A. Milanes[77,z], A. Minotti[31,p], E. Minucci[28], T. Miralles[11], B. Mitreska[19], D. S. Mitzel[19], R. Mocanu[43], A. Modak[58], L. Moeser[19], R. D. Moise[17], E. F. Molina Cardenas[87], T. Mombächer[49], M. Monk[1,57], S. Monteil[11], A. Morcillo Gomez[47], G. Morello[28], M. J. Morello[35,t], M. P. Morgenthaler[22], A. Moro[31,p], J. Moron[40], W. Morren[38], A. B. Morris[49], A. G. Morris[13], R. Mountain[69], H. Mu[4,d], Z. M. Mu[6], E. Muhammad[57], F. Muheim[59], M. Mulder[81], K. Müller[51], F. Muñoz-Rojas[9], R. Murta[62], V. Mytrochenko[52], P. Naik[61], T. Nakada[50], R. Nandakumar[58], T. Nanut[49], I. Nasteva[3], M. Needham[59], E. Nekrasova[44], N. Neri[30,o], S. Neubert[18], N. Neufeld[49], P. Neustroev[44], J. Nicolini[49], D. Nicotra[82], E. M. Niel[15], N. Nikitin[44], L. Nisi[19], Q. Niu[74], P. Nogarolli[3], P. Nogga[18], C. Normand[55], J. Novoa Fernandez[47], G. Nowak[66], C. Nunez[87], H. N. Nur[60], A. Oblakowska-Mucha[40], V. Obraztsov[44], T. Oeser[17], A. Okhotnikov[44], O. Okhrimenko[53], R. Oldeman[32,l], F. Oliva[59,49], E. Olivart Pino[45], M. Olocco[19], C. J. G. Onderwater[82], R. H. O'Neil[49], J. S. Ordonez Soto[11], D. Osthues[19], J. M. Otalora Goicochea[3], P. Owen[51], A. Oyanguren[48], O. Ozcelik[49], F. Paciolla[35,x], A. Padee[42], K. O. Padeken[18], B. Pagare[47], T. Pajero[49], A. Palano[24], L. Palini[30], M. Palutan[28], C. Pan[75], X. Pan[4,d], S. Panebianco[12], G. Panshin[5], L. Paolucci[63], A. Papanestis[58], M. Pappagallo[24,i], L. L. Pappalardo[26], C. Pappenheimer[66], C. Parkes[63], D. Parmar[78], B. Passalacqua[26,m], G. Passaleva[27], D. Passaro[35,49,t], A. Pastore[24], M. Patel[62], J. Patoc[64], C. Patrignani[25,k], A. Paul[69], C. J. Pawley[82], A. Pellegrino[38], J. Peng[5,7], X. Peng[74], M. Pepe Altarelli[28], S. Perazzini[25], D. Pereima[44], H. Pereira Da Costa[68], M. Pereira Martinez[47], A. Pereiro Castro[47], C. Perez[46], P. Perret[11], A. Perrevoort[81], A. Perro[13,49], M. J. Peters[66], K. Petridis[55], A. Petrolini[29,n], S. Pezzulo[29,n], J. P. Pfaller[66],

H. Pham[69], L. Pica[35,t], M. Piccini[34], L. Piccolo[32], B. Pietrzyk[10], G. Pietrzyk[14], R. N. Pilato[61], D. Pinci[36], F. Pisani[49], M. Pizzichemi[31,49,p], V. M. Placinta[43], M. Plo Casasus[47], T. Poeschl[49], F. Polci[16], M. Poli Lener[28], A. Poluektov[13], N. Polukhina[44], I. Polyakov[63], E. Polycarpo[3], S. Ponce[49], D. Popov[7,49], S. Poslavskii[44], K. Prasanth[59], C. Prouve[84], D. Provenzano[32,49,l], V. Pugatch[53], G. Punzi[35,u], J. R. Pybus[68], S. Qasim[51], Q. Q. Qian[6], W. Qian[7], N. Qin[4,d], S. Qu[4,d], R. Quagliani[49], R. I. Rabadan Trejo[57], R. Racz[80], J. H. Rademacker[55], M. Rama[35], M. Ramírez García[87], V. Ramos De Oliveira[70], M. Ramos Pernas[57], M. S. Rangel[3], F. Ratnikov[44], G. Raven[39], M. Rebollo De Miguel[48], F. Redi[30,j], J. Reich[55], F. Reiss[20], Z. Ren[7], P. K. Resmi[64], M. Ribalda Galvez[45], R. Ribatti[50], G. Ricart[12,15], D. Riccardi[35,t], S. Ricciardi[58], K. Richardson[65], M. Richardson-Slipper[56], K. Rinnert[61], P. Robbe[14,49], G. Robertson[60], E. Rodrigues[61], A. Rodriguez Alvarez[45], E. Rodriguez Fernandez[47], J. A. Rodriguez Lopez[77], E. Rodriguez Rodriguez[49], J. Roensch[19], A. Rogachev[44], A. Rogovskiy[58], D. L. Rolf[19], P. Roloff[49], V. Romanovskiy[66], A. Romero Vidal[47], G. Romolini[26,49], F. Ronchetti[50], T. Rong[6], M. Rotondo[28], S. R. Roy[22], M. S. Rudolph[69], M. Ruiz Diaz[22], R. A. Ruiz Fernandez[47], J. Ruiz Vidal[82], J. J. Saavedra-Arias[9], J. J. Saborido Silva[47], S. E. R. Sacha Emile R.[49], N. Sagidova[44], D. Sahoo[79], N. Sahoo[54], B. Saitta[32,l], M. Salomoni[31,49,p], I. Sanderswood[48], R. Santacesaria[36], C. Santamarina Rios[47], M. Santimaria[28], L. Santoro[2], E. Santovetti[37], A. Saputi[26,49], D. Saranin[44], A. Sarnatskiy[81], G. Sarpis[49], M. Sarpis[80], C. Satriano[36,v], M. Saur[74], D. Savrina[44], H. Sazak[17], F. Sborzacchi[28,49], A. Scarabotto[19], S. Schael[17], S. Scherl[61], M. Schiller[22], H. Schindler[49], M. Schmelling[21], B. Schmidt[49], N. Schmidt[68], S. Schmitt[65], H. Schmitz[18], O. Schneider[50], A. Schopper[62], N. Schulte[19], M. H. Schune[14], G. Schwering[17], B. Sciascia[28], A. Sciuccati[49], G. Scriven[82], I. Segal[78], S. Sellam[47], A. Semennikov[44], T. Senger[51], M. Senghi Soares[39], A. Sergi[29,49,n], N. Serra[51], L. Sestini[27], A. Seuthe[19], B. Sevilla Sanjuan[46], Y. Shang[6], D. M. Shangase[87], M. Shapkin[44], R. S. Sharma[69], I. Shchemerov[44], L. Shchutska[50], T. Shears[61], L. Shekhtman[44], Z. Shen[38], S. Sheng[5,7], V. Shevchenko[44], B. Shi[7], Q. Shi[7], W. S. Shi[73], Y. Shimizu[14], E. Shmanin[25], R. Shorkin[44], J. D. Shupperd[69], R. Silva Coutinho[2], G. Simi[33,r], S. Simone[24,i], M. Singha[79], N. Skidmore[57], T. Skwarnicki[69], M. W. Slater[54], E. Smith[65], K. Smith[68], M. Smith[62], L. Soares Lavra[59], M. D. Sokoloff[66], F. J. P. Soler[60], A. Solomin[55], A. Solovev[44], K. Solovieva[20], N. S. Sommerfeld[18], R. Song[1], Y. Song[50], Y. Song[4,d], Y. S. Song[6], F. L. Souza De Almeida[69], B. Souza De Paula[3], E. Spadaro Norella[29,n], E. Spedicato[25], J. G. Speer[19], P. Spradlin[60], V. Sriskaran[49], F. Stagni[49], M. Stahl[78], S. Stahl[49], S. Stanislaus[64], M. Stefaniak[88], E. N. Stein[49], O. Steinkamp[51], H. Stevens[19], D. Strekalina[44], Y. Su[7], F. Suljik[64], J. Sun[32], J. Sun[63], L. Sun[75], D. Sundfeld[2], W. Sutcliffe[51], V. Svintozelskyi[48], K. Swientek[40], F. Swystun[56], A. Szabelski[42], T. Szumlak[40], Y. Tan[4,d], Y. Tang[75], Y. T. Tang[7], M. D. Tat[22], J. A. Teijeiro Jimenez[47], A. Terentev[44], F. Terzuoli[35,x], F. Teubert[49], E. Thomas[49], D. J. D. Thompson[54], A. R. Thomson-Strong[59], H. Tilquin[62], V. Tisserand[11], S. T'Jampens[10], M. Tobin[5], T. T. Todorov[20], L. Tomassetti[26,m], G. Tonani[30], X. Tong[6], T. Tork[30], D. Torres Machado[2], L. Toscano[19], D. Y. Tou[4,d], C. Trippl[46], G. Tuci[22], N. Tuning[38], L. H. Uecker[22], A. Ukleja[40], D. J. Unverzagt[22], A. Upadhyay[49], B. Urbach[59], A. Usachov[39], A. Ustyuzhanin[44], U. Uwer[22], V. Vagnoni[25], V. Valcarce Cadenas[47], G. Valenti[25], N. Valls Canudas[49], J. van Eldik[49], H. Van Hecke[68], E. van Herwijnen[62], C. B. Van Hulse[47,aa], R. Van Laak[50], M. van Veghel[38], G. Vasquez[51], R. Vazquez Gomez[45], P. Vazquez Regueiro[47], C. Vázquez Sierra[84], S. Vecchi[26], J. Velilla Serna[48], J. J. Velthuis[55], M. Veltri[27,y], A. Venkateswaran[50], M. Verdoglia[32], M. Vesterinen[57], W. Vetens[69], D. Vico Benet[64], P. Vidrier Villalba[45], M. Vieites Diaz[47,49], X. Vilasis-Cardona[46], E. Vilella Figueras[61], A. Villa[25], P. Vincent[16], B. Vivacqua[3], F. C. Volle[54], D. vom Bruch[13], N. Voropaev[44], K. Vos[82], C. Vrahas[59], J. Wagner[19], J. Walsh[35], E. J. Walton[1,57], G. Wan[6], A. Wang[7], B. Wang[5], C. Wang[22], G. Wang[8], H. Wang[74], J. Wang[6], J. Wang[5], J. Wang[4,d], J. Wang[75], M. Wang[49], N. W. Wang[7], R. Wang[55], X. Wang[8], X. Wang[73], X. W. Wang[62], Y. Wang[76], Y. Wang[6], Y. H. Wang[74], Z. Wang[14], Z. Wang[30], J. A. Ward[57], M. Waterlaat[49], N. K. Watson[54], D. Websdale[62], Y. Wei[6], Z. Weida[7], J. Wendel[84], B. D. C. Westhenry[55], C. White[56], M. Whitehead[60], E. Whiter[54], A. R. Wiederhold[63], D. Wiedner[19], M. A. Wiegertjes[38], C. Wild[64], G. Wilkinson[49,64], M. K. Wilkinson[66], M. Williams[65], M. J. Williams[49], M. R. J. Williams[59], R. Williams[56], S. Williams[55], Z. Williams[55], F. F. Wilson[58], M. Winn[12], W. Wislicki[42], M. Witek[41], L. Witola[19], T. Wolf[22], E. Wood[56], G. Wormser[14], S. A. Wotton[56], H. Wu[69], J. Wu[8], X. Wu[75], Y. Wu[6,56], Z. Wu[7], K. Wyllie[49], S. Xian[73], Z. Xiang[5], Y. Xie[8], T. X. Xing[30], A. Xu[35,t], L. Xu[4,d], L. Xu[4,d], M. Xu[49], Z. Xu[49], Z. Xu[7], Z. Xu[5], K. Yang[62], X. Yang[6], Y. Yang[15], Y. Yang[79], Z. Yang[6], V. Yeroshenko[14], H. Yeung[63], H. Yin[8], X. Yin[7], C. Y. Yu[6], J. Yu[72], X. Yuan[5], Y Yuan[5,7], E. Zaffaroni[50], J. A. Zamora Saa[71], M. Zavertyaev[21],

M. Zdybal[41], F. Zenesini[25], C. Zeng[5,7], M. Zeng[4,d], C. Zhang[6], D. Zhang[8], J. Zhang[7], L. Zhang[4,d], R. Zhang[8], S. Zhang[72], S. Zhang[64], Y. Zhang[6], Y. Z. Zhang[4,d], Z. Zhang[4,d], Y. Zhao[22], A. Zhelezov[22], S. Z. Zheng[6], X. Z. Zheng[4,d], Y. Zheng[7], T. Zhou[6], X. Zhou[8], Y. Zhou[7], V. Zhovkovska[57], L. Z. Zhu[7], X. Zhu[4,d], X. Zhu[8], Y. Zhu[17], V. Zhukov[17], J. Zhuo[48], Q. Zou[5,7], D. Zuliani[33,r], G. Zunica[28]

[1] School of Physics and Astronomy, Monash University, Melbourne, Australia
[2] Centro Brasileiro de Pesquisas Físicas (CBPF), Rio de Janeiro, Brazil
[3] Universidade Federal do Rio de Janeiro (UFRJ), Rio de Janeiro, Brazil
[4] Department of Engineering Physics, Tsinghua University, Beijing, China
[5] Institute of High Energy Physics (IHEP), Beijing, China
[6] School of Physics State Key Laboratory of Nuclear Physics and Technology, Peking University, Beijing, China
[7] University of Chinese Academy of Sciences, Beijing, China
[8] Institute of Particle Physics, Central China Normal University, Wuhan, Hubei, China
[9] Consejo Nacional de Rectores (CONARE), San Jose, Costa Rica
[10] Université Savoie Mont Blanc, CNRS, IN2P3-LAPP, Annecy, France
[11] Université Clermont Auvergne, CNRS/IN2P3, LPC, Clermont-Ferrand, France
[12] Université Paris-Saclay, Centre d'Etudes de Saclay (CEA), IRFU, Saclay, Gif-Sur-Yvette, France
[13] Aix Marseille Univ, CNRS/IN2P3, CPPM, Marseille, France
[14] Université Paris-Saclay, CNRS/IN2P3, IJCLab, Orsay, France
[15] Laboratoire Leprince-Ringuet, CNRS/IN2P3, Ecole Polytechnique, Institut Polytechnique de Paris, Palaiseau, France
[16] LPNHE, Sorbonne Université, Paris Diderot Sorbonne Paris Cité, CNRS/IN2P3, Paris, France
[17] I. Physikalisches Institut, RWTH Aachen University, Aachen, Germany
[18] Universität Bonn-Helmholtz-Institut für Strahlen und Kernphysik, Bonn, Germany
[19] Fakultät Physik, Technische Universität Dortmund, Dortmund, Germany
[20] Physikalisches Institut, Albert-Ludwigs-Universität Freiburg, Freiburg, Germany
[21] Max-Planck-Institut für Kernphysik (MPIK), Heidelberg, Germany
[22] Physikalisches Institut, Ruprecht-Karls-Universität Heidelberg, Heidelberg, Germany
[23] School of Physics, University College Dublin, Dublin, Ireland
[24] INFN Sezione di Bari, Bari, Italy
[25] INFN Sezione di Bologna, Bologna, Italy
[26] INFN Sezione di Ferrara, Ferrara, Italy
[27] INFN Sezione di Firenze, Florence, Italy
[28] INFN Laboratori Nazionali di Frascati, Frascati, Italy
[29] INFN Sezione di Genova, Genoa, Italy
[30] INFN Sezione di Milano, Milan, Italy
[31] INFN Sezione di Milano-Bicocca, Milan, Italy
[32] INFN Sezione di Cagliari, Monserrato, Italy
[33] INFN Sezione di Padova, Padua, Italy
[34] INFN Sezione di Perugia, Perugia, Italy
[35] INFN Sezione di Pisa, Pisa, Italy
[36] INFN Sezione di Roma La Sapienza, Rome, Italy
[37] INFN Sezione di Roma Tor Vergata, Rome, Italy
[38] Nikhef National Institute for Subatomic Physics, Amsterdam, The Netherlands
[39] Nikhef National Institute for Subatomic Physics and VU University Amsterdam, Amsterdam, The Netherlands
[40] Faculty of Physics and Applied Computer Science, AGH-University of Krakow, Cracow, Poland
[41] Henryk Niewodniczanski Institute of Nuclear Physics Polish Academy of Sciences, Cracow, Poland
[42] National Center for Nuclear Research (NCBJ), Warsaw, Poland
[43] Horia Hulubei National Institute of Physics and Nuclear Engineering, Bucharest-Magurele, Romania
[44] Authors Affiliated with an Institute Formerly Covered by a Cooperation Agreement with CERN, Geneva, Switzerland
[45] ICCUB, Universitat de Barcelona, Barcelona, Spain
[46] La Salle, Universitat Ramon Llull, Barcelona, Spain
[47] Instituto Galego de Física de Altas Enerxías (IGFAE), Universidade de Santiago de Compostela, Santiago de Compostela, Spain

[48] Instituto de Fisica Corpuscular, Centro Mixto Universidad de Valencia-CSIC, Valencia, Spain
[49] European Organization for Nuclear Research (CERN), Geneva, Switzerland
[50] Institute of Physics, Ecole Polytechnique Fédérale de Lausanne (EPFL), Lausanne, Switzerland
[51] Physik-Institut, Universität Zürich, Zürich, Switzerland
[52] NSC Kharkiv Institute of Physics and Technology (NSC KIPT), Kharkiv, Ukraine
[53] Institute for Nuclear Research of the National Academy of Sciences (KINR), Kyiv, Ukraine
[54] School of Physics and Astronomy, University of Birmingham, Birmingham, UK
[55] H. H. Wills Physics Laboratory, University of Bristol, Bristol, UK
[56] Cavendish Laboratory, University of Cambridge, Cambridge, UK
[57] Department of Physics, University of Warwick, Coventry, UK
[58] STFC Rutherford Appleton Laboratory, Didcot, UK
[59] School of Physics and Astronomy, University of Edinburgh, Edinburgh, UK
[60] School of Physics and Astronomy, University of Glasgow, Glasgow, UK
[61] Oliver Lodge Laboratory, University of Liverpool, Liverpool, UK
[62] Imperial College London, London, UK
[63] Department of Physics and Astronomy, University of Manchester, Manchester, UK
[64] Department of Physics, University of Oxford, Oxford, UK
[65] Massachusetts Institute of Technology, Cambridge, MA, USA
[66] University of Cincinnati, Cincinnati, OH, USA
[67] University of Maryland, College Park, MD, USA
[68] Los Alamos National Laboratory (LANL), Los Alamos, NM, USA
[69] Syracuse University, Syracuse, NY, USA
[70] Pontifícia Universidade Católica do Rio de Janeiro (PUC-Rio), Rio de Janeiro, Brazil
[71] Universidad Andres Bello, Santiago, Chile associated to [51]
[72] School of Physics and Electronics, Hunan University, Changsha City, China associated to [8]
[73] Guangdong Provincial Key Laboratory of Nuclear Science, Guangdong-Hong Kong Joint Laboratory of Quantum Matter, Institute of Quantum Matter, South China Normal University, Guangzhou, China
[74] Lanzhou University, Lanzhou, China associated to [5]
[75] School of Physics and Technology, Wuhan University, Wuhan, China associated to [4]
[76] Henan Normal University, Xinxiang, China associated to [8]
[77] Departamento de Fisica, Universidad Nacional de Colombia, Bogota, Colombia associated to [16]
[78] Ruhr Universitaet Bochum, Fakultaet f. Physik und Astronomie, Bochum, Germany associated to [19]
[79] Eotvos Lorand University, Budapest, Hungary associated to [49]
[80] Faculty of Physics, Vilnius University, Vilnius, Lithuania associated to [20]
[81] Van Swinderen Institute, University of Groningen, Groningen, The Netherlands associated to [38]
[82] Universiteit Maastricht, Maastricht, The Netherlands associated to [38]
[83] Tadeusz Kosciuszko Cracow University of Technology, Cracow, Poland associated to [41]
[84] Universidade da Coruña, A Coruña, Spain associated to [46]
[85] Department of Physics and Astronomy, Uppsala University, Uppsala, Sweden associated to [60]
[86] Faculty of Physics, Taras Schevchenko University of Kyiv, Kyiv, Ukraine associated to [14]
[87] University of Michigan, Ann Arbor, MI, USA associated to [69]
[88] Ohio State University, Columbus, USA associated to [68]

[a] Universidade Estadual de Campinas (UNICAMP), Campinas, Brazil
[b] Centro Federal de Educacão Tecnológica Celso Suckow da Fonseca, Rio de Janeiro, Brazil
[c] Department of Physics and Astronomy, University of Victoria, Victoria, Canada
[d] Center for High Energy Physics, Tsinghua University, Beijing, China
[e] Hangzhou Institute for Advanced Study, UCAS, Hangzhou, China
[f] LIP6, Sorbonne Université, Paris, France
[g] Lamarr Institute for Machine Learning and Artificial Intelligence, Dortmund, Germany
[h] Universidad Nacional Autónoma de Honduras, Tegucigalpa, Honduras
[i] Università di Bari, Bari, Italy
[j] Università di Bergamo, Bergamo, Italy

[k] Università di Bologna, Bologna, Italy
[l] Università di Cagliari, Cagliari, Italy
[m] Università di Ferrara, Ferrara, Italy
[n] Università di Genova, Genoa, Italy
[o] Università degli Studi di Milano, Milan, Italy
[p] Università degli Studi di Milano-Bicocca, Milan, Italy
[q] Università di Modena e Reggio Emilia, Modena, Italy
[r] Università di Padova, Padua, Italy
[s] Università di Perugia, Perugia, Italy
[t] Scuola Normale Superiore, Pisa, Italy
[u] Università di Pisa, Pisa, Italy
[v] Università della Basilicata, Potenza, Italy
[w] Università di Roma Tor Vergata, Rome, Italy
[x] Università di Siena, Siena, Italy
[y] Università di Urbino, Urbino, Italy
[z] Universidad de Ingeniería y Tecnología (UTEC), Lima, Peru
[aa] Universidad de Alcalá, Alcalá de Henares , Spain
*Deceased